IEEE Access
Multidisciplinary | Rapid Review | Open Access Journal

Received July 26, 2020, accepted August 8, 2020, date of publication August 17, 2020, date of current version August 26, 2020.

Digital Object Identifier 10.1109/ACCESS.2020.3016147

A Photonic Digitization Scheme With Enhanced Bit Resolution Based on Hierarchical Quantization

SHUNA YANG, ZHIWEI LIU, HAO CHI, (Senior Member, IEEE), RAN ZENG, AND BO YANG
School of Communication Engineering, Hangzhou Dianzi University, Hangzhou 310018, China

Corresponding author: Hao Chi (chihao@hdu.edu.cn)

This work was supported in part by the National Key Research and Development Program of China under Grant 2019YFB2203204, in part by the National Natural Science Foundation of China under Grant 61901148, Grant 61975048, Grant 11574068, and Grant 41905024; in part by the Zhejiang Provincial Natural Science Foundation under Grant LQ18F050002 and Grant LZ20F010003, and in part by the Foundation of Zhejiang Education Committee under Grant Y201635688.

ABSTRACT The major limitation of the photonic digitization schemes based on the phase-shifting of modulation transfer function lies in its relatively low bit resolution, which is $\log_2(2N)$, where N is the number of optical channels or modulators. In this paper, we propose a novel photonic digitization scheme based on hierarchical quantization, which could greatly improve the system resolution with a relatively simple configuration. It is shown that $6N$ quantization levels, can be realized by using only three Mach-Zehnder modulators (MZMs) and a hierarchical quantization module (HQM) in the proposed scheme. By adjusting the fine quantization module inside HQM, the system resolution can be enhanced greatly. A proof-of-concept experiment is implemented, which fully verifies the correctness of the approach. Since simpler configuration and higher resolution are achieved, the proposed scheme provides a promising solution for high-performance photonic analog-to-digital conversion.

INDEX TERMS Analog-to-digital conversion, hierarchical quantization, ENOB.

I. INTRODUCTION

The wideband signal acquisition, such as wideband radars, electronic monitor, high-speed optical and wireless communications, requires high performance analog-to-digital conversion (ADC) [1]–[3]. However, limited by the inherent aperture jitter of sampling clock and comparator ambiguity, it is a big challenge for the current electronic ADCs to digitize analog signals with a sampling rate over tens of gigahertz while keeping high resolution [4]. Benefiting from the ultra-wide bandwidth and electromagnetic interference immunity offered by photonic components as well as the ultra-low jitter of mode-locked lasers, photonics-assisted ADC is widely regarded as a promising candidate to break the bottleneck of electronic digitization in bandwidth and resolution [5]. In the past several decades, many ADC schemes with the help of photonic technologies have been proposed. Typical schemes include the techniques of photonic sampling and electronic digitizing [6], [7], the technique of photonic time stretch for preprocessing signals prior to electronic quantization [8], [9], the approaches based on amplitude-to-frequency conversion using optical nonlinearities [10], [11], and the photonic digitization schemes using Mach-Zehnder interferometers (MZIs) or Mach-Zehnder modulators (MZMs) [12]–[18], as well as others [19], [20].

Taylor proposed a photonic digitization scheme based on an MZM array in 1970s, which employs the sinusoidal modulation transfer functions of MZMs to quantize the input analog signal [12]. In this approach, the digital output is Gray code and the bit resolution is equal to the number of MZMs. However, the achievable system resolution is limited by the geometrically scaled half-wave voltages (V_π) of employed MZMs, e.g., for a 4-bit system, V_π of the MZM for the least significant bit (LSB) is 1/16 of that for the most significant bit (MSB), which is hard to realize even with the state-of-art photonic fabrication techniques. In order to overcome this limitation, Stigwall *et al.* put forward a photonic digitization scheme based on the phase-shifting of the modulation transfer function of an MZI, which was realized by using a free-space MZI with a phase modulator (PM) in one arm and placing photodetectors (PDs) at different positions in the interference pattern [13]. Since this approach avoids the difficulty relating to V_π scaling as in Taylor's approach, the concept of phase-shifting photonic digitization (PSPD) has attracted a great deal of attention. Up to now a number of PSPD schemes have been proposed, such as the approach using a PM and polarization interferometric phase shifters [14], the scheme using properly biased MZMs with identical V_π [15], the

The associate editor coordinating the review of this manuscript and approving it for publication was Weiren Zhu.

differential encoding scheme using a single PM and delay line interferometers [16], the approach using an unbalanced MZM [17], and so on [18]. Although the PSPD schemes avoid the geometrical scaling of V_π, the realized quantization levels are relatively low, which is $2N$ for a system with N channels but not 2^N as in Taylor's scheme. Accordingly, the bit resolution is $\log_2(2N)$, which is much lower than N bits when $N > 2$. Hence, how to improve the bit resolution is a major issue for the PSPD schemes. Some efforts have been made to enhance the bit resolution of PSPD scheme, which include the technique of the symmetrical number system (SNS) [21], the approach using electrical circuits for linear combination [22], the method with cascaded quantization modules [23], as well as the scheme based on signal rectification [24]. However, these solutions improve the system bit resolution at the cost of huge number of comparators [21], the complicated logic circuits [22], specially designed MZMs with cascaded optical couplers [23], or wideband signal rectifiers [24]. Therefore, it is still an open question to find a relatively simple design of PSPD schemes with improved bit resolution.

In this paper, we propose and demonstrate a novel photonic digitization scheme based on hierarchical quantization, which greatly improves the bit resolution with a much simpler configuration. The scheme employs three parallel MZMs with identical V_π and a hierarchical quantization module (HQM). The MZMs are properly biased to achieve the desired phase shifts among different transfer functions. The HQM is used to quantize the modulated signals out of the MZMs. With the help of HQM, $6N$ levels can be obtained, which is much greater than previous PSPD schemes with the same number of MZMs. Accordingly, the bit resolution is enhanced from $\log_2(6)$ to $\log_2(6N)$. Moreover, compared with the previous resolution-enhanced ADC schemes, the proposed scheme features less complexity since only 3 MZMs and an HQM are required. We implement a proof-of-concept experiment of a system with 18 quantization levels to verify the correctness and feasibility of the approach. We also present a comparison of the required number of MZMs and comparators among the proposed scheme and other typical PSPD schemes.

II. PRINCIPLE OF OPERATION

A schematic diagram of the proposed photonic digitization scheme based on hierarchical quantization is shown in Fig. 1(a). The system consists of a mode-locked laser, three MZMs with identical V_π, a hierarchical quantization module (HQM), and a combining logic module. An optical pulse train from the mode-locked laser is sent to three parallel MZMs via an optical coupler to sample the input radio frequency (RF) signal, which is applied to the MZMs via RF ports. The modulated pulse train from the parallel MZMs is then delivered to the HQM to perform quantization and encoding. The output of HQM is the thermometer code, which is converted into the ordinary binary code by the following combining logic module. In order to achieve the desired phase shifts among three modulation transfer functions, the MZMs are properly

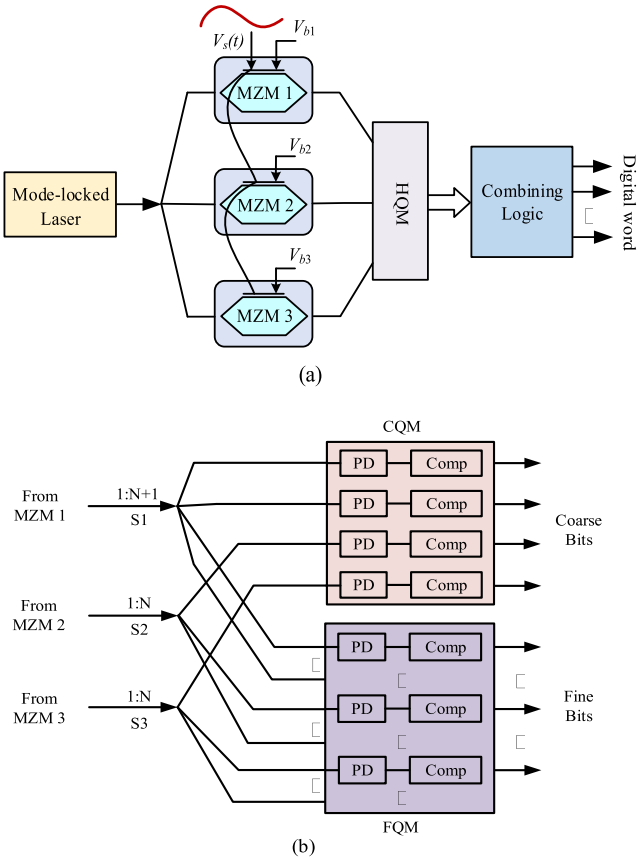

FIGURE 1. (a) Schematic diagram of the proposed digitization scheme; (b) the configuration of the hierarchical quantization module. MZM: Mach-Zehnder modulator. HQM: hierarchical quantization module. CQM: coarse quantization module. FQM: fine quantization module. PD: photo-detector. Comp: comparator.

biased by adjusting the applied bias voltages. The detailed configuration of the HQM is shown in Fig. 1(b). It consists of three optical splitters, a coarse quantization module (CQM) and a fine quantization module (FQM). Both the CQM and FQM consist of PDs and comparators.

The modulated pulse trains from MZM2 and MZM3 are split into N (i.e. the number of optical paths split from S2 or S3) paths by S2 and S3, respectively. The first paths from both S2 and S3 are connected to the CQM, the remaining $N - 1$ paths are connected to the FQM. The modulated pulse train from MZM1 is split into $N + 1$ paths by the splitter 1 (S1). The first two paths out of S1 are connected to the CQM, and the remaining $N - 1$ paths are connected to the FQM. There is a PD in each path for O/E conversion. The following comparator generates the digital code by comparing the detected electrical signal with the preset threshold value.

In the scheme, the modulated signals from the three MZMs are quantized in two stages by the HQM. The first stage is the coarse quantization performed by the CQM, which quantizes the input signal into 6 levels. Coarse bits shown in Fig. 1(b) denote the digital code output of CQM. The second stage is the fine quantization realized by the FQM, which further quantizes each level obtained from the CQM. Fine bits in Fig. 1(b) denote the digital code generated by FQM.

Benefitting from the FQM, each of 6 CQM quantization levels is further divided into N levels. Accordingly, the number of total quantization levels is enhanced from 6 to $6N$.

In the proposed scheme, the output optical intensity from the i-th MZM ($i = 1, 2, 3$) is given by

$$I_i = \frac{I_0}{2}\{1 + \cos[\varphi_d(t) + \varphi_i]\} \tag{1}$$

where I_0 is the input optical intensity, $\varphi_d(t) = \pi V_s(t)/V_\pi$ is the phase shift induced by the applied analog signal $V_s(t)$, V_π is the half-wave voltage of the MZMs, $\varphi_i = \pi V_{bi}/V_\pi$ is the phase shift induced by the bias voltage V_{bi} applied to the i-th MZM. To get a uniform quantization, the bias voltages applied to the MZMs should be properly adjusted to guarantee a difference of $\pi/3$ between adjacent φ_i. For simplicity, we assume the bias phase shift φ_i of the three MZMs as 0, $\pi/3$ and $2\pi/3$. The modulated signals from the three MZMs are split into $N+1$, N and N paths by S1, S2 and S3, respectively. We denote the j-th ($1 \le j \le N+1$) path out of S1 as c_{1j}, the j-th ($1 \le j \le N$) path from S2 as c_{2j}, and that following S3 as c_{3j}, then c_{11}, c_{12}, c_{21} and c_{31} are connected to the CQM to perform the coarse quantization. By setting the normalized threshold values of comparators in paths c_{11}, c_{12}, c_{21}, c_{31} as 0.75, 0.25, 0.25 and 0.25, respectively, the CQM quantizes the input signal into 6 levels. The FQM performs the further quantization of each level obtained by the CQM. The optical signals sent to the FQM are digitized by the following comparators. The threshold value of the comparator in k-th ($k = 1, 2, \cdots, N-1$) path following the i-th splitter is set as

$$T_{ik} = \frac{1}{2}[1 + \cos(\pi V_k/V_\pi)] \tag{2}$$

where $V_k = V_\pi(N + k)/3N$. We assume that the signal intensity greater than the threshold value is digitized as "1", otherwise it is digitized as "0". Note that in CQM, the signals out of MZM1 are digitized based on the threshold values of c_{11} and c_{12}, while those of MZM2 and MZM3 are compared with c_{21} and c_{31} respectively.

The detailed quantization and encoding process of a digitization system with quantization levels of 18 ($N = 3$) is shown in Fig. 2. A simulation model built by Matlab is used to verify the proposed photonic digitization scheme. The input analog signal $V_s(t)$ is assumed to be a sinusoidal signal with the bandwidth of 4 GHz. The output time-domain signals from the three MZMs are shown in Fig. 2(a). Fig. 2(b) gives the modulation transfer functions of the three MZMs and the quantization/encoding process of the CQM, where the horizontal axis denotes the phase signal $\varphi_d(t)$ induced by the RF signal and the vertical axis indicates the normalized intensity of the output optical signal. The normalized threshold values of the four paths are set as 0.75 (c_{11}), 0.25 (c_{21}), 0.25 (c_{22}) and 0.25 (c_{31}), respectively. By comparing the signal intensity with the preset threshold values, the digital output is obtained. From Fig. 2(b), it is seen that 6 quantization levels can be obtained by the CQM, which are expressed in the form of the digital words as [011, 111, 211, 210, 100, 001].

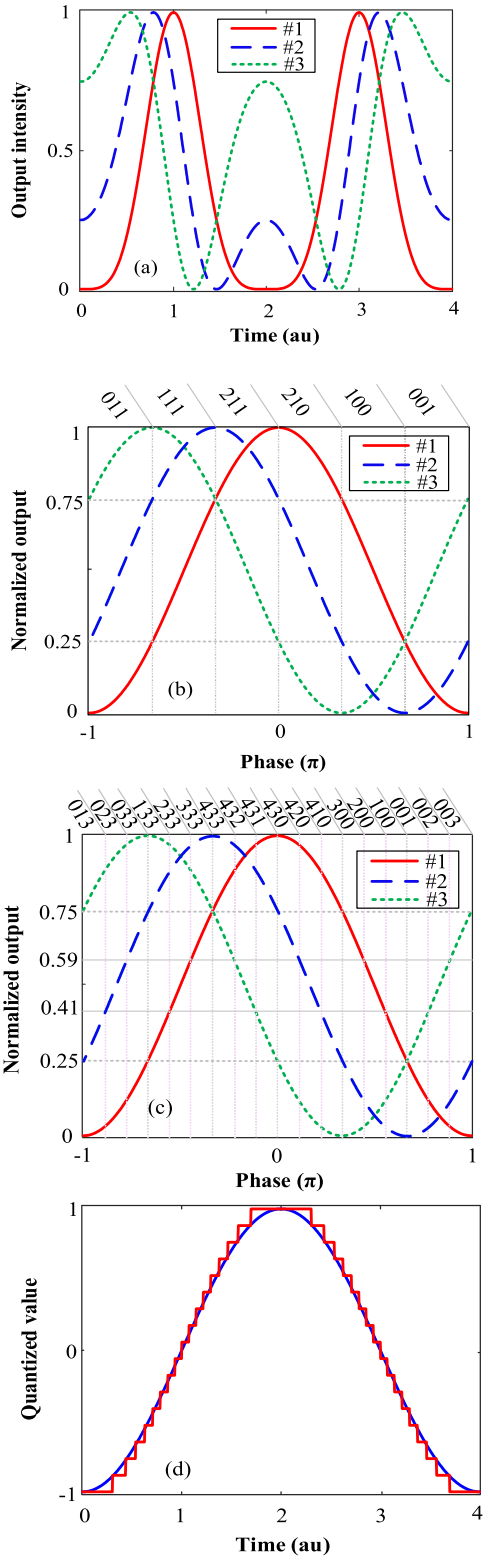

FIGURE 2. Quantization process of the proposed photonic digitization system. (a) The normalized output signal intensities of three MZMs. (b) The quantization and encoding in CQM. (c) The quantization and encoding in HQM with 18 levels. (d) The quantized values and the sinusoidal fitted curve.

Note that the digit in the code represents the total number of output "1". Then, two paths from each splitter are connected

to the FQM, the normalized threshold values are set to be $T_{11} = 0.59, T_{12} = 0.41, T_{21} = 0.59, T_{22} = 0.41, T_{31} = 0.59$ and $T_{32} = 0.41$. The quantization and encoding process of the FQM is shown in Fig. 2(c). Since all threshold values (for both CQM and FQM) are used for encoding, the digital code shown in Fig. 2(c) denote that output of HQM, and it will be delivered to the following combing logic to achieve the ordinary digital code. Obviously, each quantization level generated by the CQM is further divided into 3 ($N = 3$) levels. Since 6 levels are achieved by the CQM, the total quantization levels achieved is 18 when $N = 3$. Based on the quantization and encoding shown in Fig. 2(b) and (c), the quantized values of the input sinusoidal signal can be obtained. Fig. 2(d) gives the quantization results as well as the input sinusoidal signal. Note that the output digital codes converted from MZM1 denote the MSB, those from MZM3 indicate LSB, and those from MZM2 denote the less significant bits. As shown in Figs. 2(b) and (c), the digital codes of the maximum and minimum amplitudes only differ in less significant bits, which are dominated by the signal from MZM2. Since the hierarchical quantization requires specific phase shifts of modulation transfer functions, the parallel MZMs should be properly biased. Especially, the error of the bias phase on MZM2 may lead to the transition between the codes corresponding to the maximum and minimum, as can be seen from Figs. 2(b) and (c).

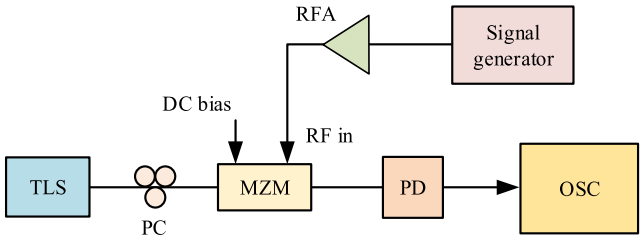

FIGURE 3. Experimental setup. TLS: tunable laser source; PC: polarization controller; MZM: Mach-Zehnder modulator; PD: photodetector; RFA: radio frequency amplifier; OSC: oscilloscope.

III. EXPERIMENT RESULTS AND DISCUSSIONS

To verify the feasibility of the proposed digitization scheme based on HQM, a proof-of-concept experiment with the setup shown in Fig. 3 is carried out, where we focus on the correctness of the quantization and encoding. A tunable laser source (HLT ITLA-C-WT) with a wavelength of 1550 nm and an output power of 8 dBm is employed as the light source. The lightwave generated by the laser source is sent to an MZM (FUJITSU FTM7937EZ200) with V_π of about 5.2 V through a polarization controller (PC). The PC is adjusted to minimize the polarization-dependent loss in the modulator. A 500 MHz sinusoidal signal, generated by a signal generator (Rohde & Schwarz SMA100B) and amplified by a radio frequency amplifier (HLT RFA-M-10-20-SMA), is used to drive the MZM, which is biased with a dc power source. A PD (DSC-R402PIN 10 GHz) is employed to implement the O/E conversion. The output temporal waveforms are observed and recorded by a 4 GHz real-time digital oscilloscope (Agilent MSO9404A). The captured waveforms are processed in an off-line program, which includes the functions of the CQM and FQM.

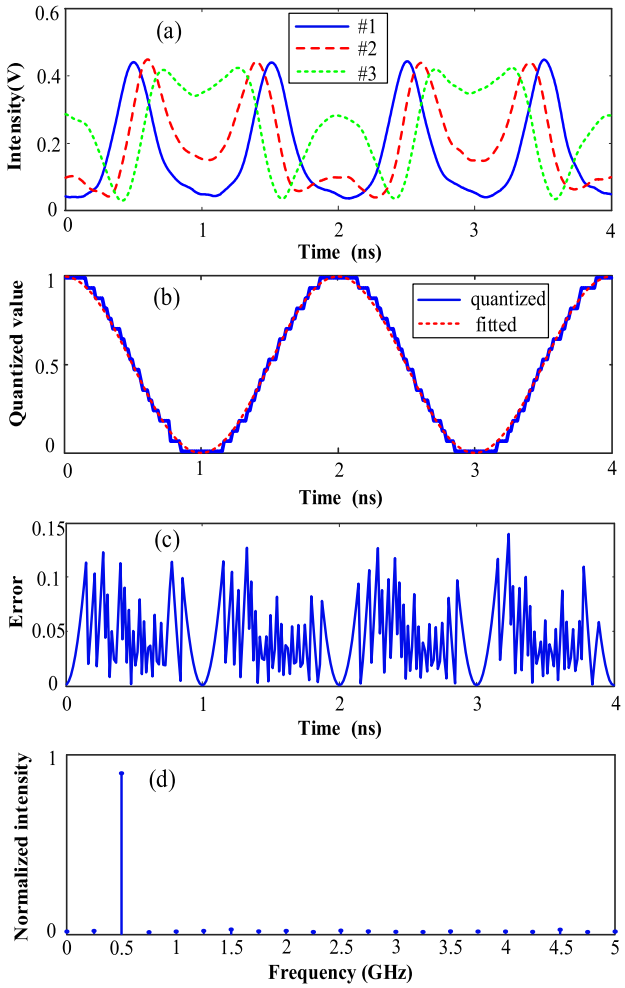

FIGURE 4. Experimental results of an 18-levels photonic digitization system. (a)The measured 3 waveforms corresponding to 3 bias phase shifts; (b) The quantized signal (solid) and the fitted sinusoidal signal(dashed); (c) Errors between the quantized and the fitted signals; (d) The spectrum of the recovered waveform.

In the experiment, we investigate a digitization system with 18 quantization levels. Limited by the available devices, we use one MZM biased at difference phase shifts to achieve the waveforms instead of three parallel MZMs. We record the output waveforms of the MZM at the bias phase shifts of 0, $V_\pi/3$ and $2V_\pi/3$, respectively, which are sufficient to verify the proposed digitization scheme. The recorded waveforms are shown in Fig. 4(a). Since the quantization levels are 18, the output signal from MZM1 is split into 4 paths and the outputs from both MZM2 and MZM3 are split into 3 paths. According to the operation principle of the HQM, 4 of 10 paths are sent to the CQM to realize the coarse quantization. The other 6 paths are sent to the FQM for fine quantization. The threshold values of both the CQM and FQM are set according to the discussions above. By comparing the sampled signal intensities with the

threshold values, the normalized digitized signal is obtained, which is shown in Fig. 4(b). For comparison, the fitted sinusoidal signal is also given. Fig. 4(c) shows the errors between the quantized and the fitted signals. Based on the errors as shown in Fig. 4(c), the digital signal-to-noise ratio (dSNR) is estimated to be around 273 (24.4 dB) and the corresponding effective number of bits (ENOB) is 3.75, according to the formula ENOB $=$ (dSNR $-$ 1.76)/6.02. It should be noted that the quantization levels of the system are 18, which corresponds to a nominal bit resolution of above 4. The ENOB deviation from the ideal case is around 0.5. The ENOB degradation is mainly owing to the errors in bias voltages and the system noise. We give the spectrum of the recovered waveform in Fig. 4(d), which also indicates the good quantization performance.

Note that in proposed scheme, three parallel MZMs are used, which means the input signal should be split to drive each MZM. In order to realize the full-scale quantization of input signal (i.e. achieve 18 quantization levels), the RF power for each MZM should be about 270 mW and the total RF power is about 810 mW. Since the splitting of the input signal will introduce the power loss, the RF power amplifier can be used to compensate the RF power loss.

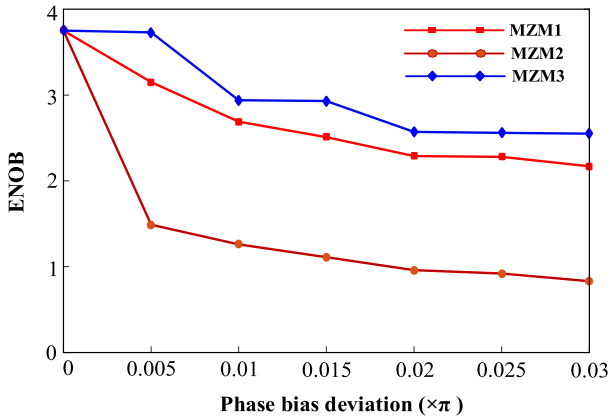

FIGURE 5. The ENOB degradation induced by the bias phase deviation.

In the proposed scheme, the parallel MZMs should be properly biased to guarantee the difference of phase shifts between any two adjacent channels as $\pi/3$. Here we focus on the impact of phase bias deviation on the system performance in terms of ENOB. We investigate the influence of the phase deviation on the ENOB in a system with 18 quantization levels. In the study, one of three MZMs is biased with the phase deviation from 0 to $0.03^{*}\pi$, and the other two MZMs are biased without error. The obtained results are shown in Fig. 5. It is seen that the ENOB decreases as the phase bias deviation increases in all cases. Furthermore, it is observed that the impact of the phase error in MZM2 is much greater than that in MZM1 or MZM3. The ENOB degrades to less than 1 bit when the phase bias deviation in MZM2 increases to $0.03^{*}\pi$. As discussed in section 2, the phase bias deviation of MZM2 may lead to the transition of the digital codes corresponding to the maximum and minimum. Therefore, the ENOB decreases very fast as the phase error increases due to the coding error. Meanwhile, since the MSB is converted from the signals out of MZM1 and the LSB is from the signals out of MZM3, the impact of the phase error in MZM1 is greater than that in MZM3. Hence, the precise control of the bias voltages applied on MZMs is vital for the proposed system. One possible implementation is to use the bias voltage holding circuit to keep the strict bias phases of MZMs.

In addition, we also estimate the optical power budget of the proposed photonic digitization system. We also consider a digitization system with 18 quantization levels, in which the modulated signals from the three MZMs are split into 10 paths. We assume the input signal is phase-modulated in full-scale, i.e. the phase shift varies from 0 to π. The responsivity and bandwidth of PD are set as 0.8 A/W and 40 GHz, respectively. We assume the system noise is dominated by the thermal noise. The insertion loss of the applied MZM is assumed to be 3 dB. If the SNR after the PDs should be greater than 30 dB, it is estimated that the optical power prior to the MZMs should be larger than 4 mW. For the systems with higher bit resolution, higher optical power is needed since that more optical channels are required inside the HQM.

IV. CONCLUSION

In this paper, a novel photonic digitization scheme with enhanced bit resolution based on hierarchical quantization was proposed and demonstrated. The hierarchical quantization module contains a coarse quantization module and a fine quantization module, both of which consist of photodetectors and comparator arrays. By properly adjusting the threshold values of the comparators inside the fine quantization module, the bit resolution of system can be dramatically improved. The principle of quantization and encoding has been described and a proof-of-concept experiment with 18 quantization levels was presented to verify the proposed scheme. We also analyzed the influence of the bias phase errors on the ENOB. In addition, we also estimate the optical power budget of the system. All obtained results show that the proposed scheme can greatly improve the bit resolution with much simpler configuration.

REFERENCES

[1] R. Llorente, M. Morant, N. Amiot, and B. Uguen, "Novel photonic analog-to-digital converter architecture for precise localization of ultra-wide band radio transmitters," *IEEE J. Sel. Areas Commun.*, vol. 29, no. 6, pp. 1321–1327, Jun. 2011.
[2] F. Su, G. Wu, and J. Chen, "Photonic analog-to-digital conversion with equivalent analog prefiltering by shaping sampling pulses," *Opt. Lett.*, vol. 41, no. 12, pp. 2779–2782, Jun. 2016.
[3] T. Nagashima, M. Hasegawa, and T. Konishi, "40 GSample/s all-optical analog to digital conversion with resolution degradation prevention," *IEEE Photon. Technol. Lett.*, vol. 29, no. 1, pp. 74–77, Jan. 1, 2017.
[4] G. C. Valley, "Photonic analog-to-digital converters," *Opt. Express*, vol. 15, no. 5, pp. 1955–1982, Mar. 2007.
[5] A. Khilo *et al.*, "Photonic ADC: Overcoming the bottleneck of electronic jitter," *Opt. Express*, vol. 20, no. 4, pp. 4454–4469, Feb. 2012.
[6] G. Yang, W. Zou, L. Yu, K. Wu, and J. Chen, "Compensation of multi-channel mismatches in high-speed high-resolution photonic analog-to-digital converter," *Opt. Express*, vol. 24, no. 21, pp. 24061–24074, Oct. 2016.

[7] F. Su, G. Wu, L. Ye, R. Liu, X. Xue, and J. Chen, "Effects of the photonic sampling pulse width and the photodetection bandwidth on the channel response of photonic ADCs," *Opt. Express*, vol. 24, no. 2, pp. 924–934, 2016.
[8] D. Peng, Z. Zhang, Y. Ma, Y. Zhang, S. Zhang, and Y. Liu, "Broadband linearization in photonic time-stretch analog-to-digital converters employing an asymmetrical dual-parallel Mach–Zehnder modulator and a balanced detector," *Opt. Express*, vol. 24, no. 11, pp. 11546–11557, May 2016.
[9] Y. Mei, Y. Xu, H. Chi, T. Jin, S. Zheng, X. Jin, and X. Zhang, "Spurious-free dynamic range of the photonic time-stretch system," *IEEE Photon. Technol. Lett.*, vol. 29, no. 10, pp. 794–797, May 15, 2017.
[10] M. Hasegawa, T. Satoh, T. Nagashima, M. Mendez, and T. Konishi, "Below 100-fs timing jitter seamless operations in 10-GSample/s 3-bit photonic Analog-to-Digital conversion," *IEEE Photon. J.*, vol. 7, no. 3, pp. 1–7, Jun. 2015.
[11] Y. Xu, T. Jin, H. Chi, S. Zheng, X. Jin, and X. Zhang, "Time-frequency uncertainty in the photonic A/D converters based on spectral encoding," *IEEE Photon. Technol. Lett.*, vol. 28, no. 8, pp. 841–844, Apr. 15, 2016.
[12] H. Taylor, "An optical analog-to-digital converter–design and analysis," *IEEE J. Quantum Electron.*, vol. QE-15, no. 4, pp. 210–216, Apr. 1979.
[13] J. Stigwall and S. Galt, "Interferometric analog-to-digital conversion scheme," *IEEE Photon. Technol. Lett.*, vol. 17, no. 2, pp. 468–470, Feb. 2005.
[14] W. Li, H. Zhang, Q. Wu, Z. Zhang, and M. Yao, "All-optical analog-to-digital conversion based on polarization-differential interference and phase modulation," *IEEE Photon. Technol. Lett.*, vol. 19, no. 8, pp. 625–627, Apr. 2007.
[15] H. Chi and J. Yao, "A photonic analog-to-digital conversion scheme using Mach–Zehnder modulators with identical half-wave voltages," *Opt. Express*, vol. 16, no. 2, pp. 567–572, Feb. 2008.
[16] H. Chi, X. Zhang, S. Zheng, X. Jin, and J. Yao, "Proposal for photonic quantization with differential encoding using a phase modulator and delay-line interferometers," *Opt. Lett.*, vol. 36, no. 9, pp. 1629–1631, May 2011.
[17] C. H. Sarantos and N. Dagli, "A photonic analog-to-digital converter based on an unbalanced Mach–Zehnder quantizer," *Opt. Express*, vol. 18, no. 14, pp. 14598–14603, Nov. 2010.
[18] X. Fu, H. Zhang, Z. Zhang, and M. Yao, "Noninterferometric optical phase-shifter module in phase-shifted optical quantization," *Opt. Eng.*, vol. 48, no. 3, Mar. 2009, Art. no. 034301.
[19] H. Hoshino, T. Okada, and M. Matsuura, "Photonic analog-to-digital conversion using a red frequency chirp in a semiconductor optical amplifier," *Opt. Lett.*, vol. 43, no. 10, pp. 2272–2275, May 2018.
[20] S. Wang, G. Wu, F. Su, and J. Chen, "Simultaneous microwave photonic analog-to-digital conversion and digital filtering," *IEEE Photon. Technol. Lett.*, vol. 30, no. 4, pp. 343–346, Feb. 15, 2018.
[21] S. Yang, C. Wang, H. Chi, X. Zhang, S. Zheng, X. Jin, and J. Yao, "Photonic analog-to-digital converter using Mach–Zehnder modulators having identical half-wave voltages with improved bit resolution," *Appl. Opt.*, vol. 48, no. 22, pp. 4458–4467, Sep. 2009.
[22] H. He, H. Chi, X. Yu, T. Jin, S. Zheng, X. Jin, and X. Zhang, "An improved photonic analog-to-digital conversion scheme using Mach–Zehnder modulators with identical half-wave voltages," *Opt. Commun.*, vol. 425, pp. 157–160, Apr. 2018.
[23] Z. Kang, X. Zhang, J. Yuan, X. Sang, Q. Wu, G. Farrell, and C. Xu, "Resolution-enhanced all-optical analog-to-digital converter employing cascade optical quantization operation," *Opt. Express*, vol. 22, no. 18, pp. 21441–21453, 2014.
[24] S. Yang, H. He, H. Chi, and R. Zeng, "A photonic quantization and encoding scheme with improved bit resolution based on waveform folding," *Opt. Express*, vol. 27, no. 24, pp. 35565–35573, Dec. 2019.

SHUNA YANG received the B.S. degree in communication engineering from Hangzhou Dianzi University, Hangzhou, China, in 2007, the M.S. degree in electronic engineering from Zhejiang University, Hangzhou, in 2010, and the Ph.D. degree in telematics from the Norwegian University of Science and Technology (NTNU), Trondheim, Norway, in 2015.

She is currently a Lecturer with the School of Communication Engineering, Hangzhou Dianzi University. She has authored or coauthored more than twenty articles in international academic journals. Her research interests include microwave photonics, optical communications, and optical networks.

ZHIWEI LIU received the B.S. degree in electronic science and information engineering from Liaocheng University, Liaocheng, China, in 2018. He is currently pursuing the master's degree with the School of Communication Engineering, Hangzhou Dianzi University, Hangzhou, China. His current research interests include microwave photonics and optical communications.

HAO CHI (Senior Member, IEEE) received the B.S. degree in applied physics from Xi'an Jiaotong University, Xi'an, China, in 1994, and the Ph.D. degree in electronic engineering from Zhejiang University, Hangzhou, China, in 2001.

From 2000 to 2001, he was a Research Assistant with The Hong Kong Polytechnic University, Hong Kong, China. From 2001 to 2003, he was a Postdoctoral Research Fellow with the Department of Electronic Engineering, Shanghai Jiao Tong University, Shanghai, China. From 2003 to 2018, he was with the College of Information Science and Electronic Engineering, Zhejiang University, where he was a Full Professor, in 2008. He is currently a Professor with the School of Communication Engineering, Hangzhou Dianzi University, Hangzhou. He has authored or coauthored more than one hundred articles in international academic journals. His research interests include microwave photonics, optical signal processing, and optical communications. He currently serves as an Associate Editor for the IEEE PHOTONICS TECHNOLOGY LETTERS.

RAN ZENG received the B.S. and Ph.D. degrees in optical physics from the Harbin Institute of Technology, Harbin, China, in 2005 and 2008, respectively. From 2012 to 2013, he was a Postdoctoral Fellow with the Laboratory of Quantum Optics and Quantum Communication, Beijing Computational Science Research Center (CSRC), Chinese Academy of Engineering Physics. From 2015 to 2016, he was a Postdoctoral Fellow with the Institute of Quantum Science and Technology, Texas A&M University. He is currently an Associate Professor with the School of Communication Engineering, Hangzhou Dianzi University, Hangzhou, China. His research interests include optical information processing, quantum optical properties of new materials, and quantum computing and information.

BO YANG received the B.S. degree in electronic information engineering and the Ph.D. degree in physical electronics from Zhejiang University, Hangzhou, China, in 2008 and 2013, respectively. From 2013 to 2017, he was a Senior Engineer with Huaxin Consulting Company, Hangzhou. From 2018 to 2019, he was a Senior Engineer with HIKVISION, Hangzhou. He is currently an Associate Professor with the School of Communication Engineering, Hangzhou Dianzi University, Hangzhou. He has authored or coauthored more than twenty articles in international academic journals. His research interests include microwave photonics, optical signal generation and processing, and next-generation optical communications and networks.